Irreversible phytoplankton community shifts over Subpolar Subpolar North Atlantic in response to CO₂ forcing

Dong-Geon Lee¹, Eun Young Kwon², Jonghun Kam¹, Jong-Seong Kug^{3,4*}

- Division of Environmental Science and Engineering, Pohang University of Science and Technology (POSTECH),
 Pohang, South Korea
 - ²IBS Center for Climate Physics, Pusan National University, Busan, South Korea
 - ³School of Earth and Environmental Sciences, Seoul National University, Seoul, South Korea
 - ⁴Interdisciplinary Program in Artificial Intelligence, Seoul National University, Seoul, South Korea

Correspondence to: Jong-Seong Kug (jskug@snu.ac.kr)

Abstract. Marine phytoplankton play a crucial role in the ocean's food web, marine ecosystems, and the carbon eyelescycle. Their responses to external forcing vary across phytoplankton species, and phytoplankton community shifts can have important implications for their roles in the Earth's system. Here, we find that phytoplankton communities in the Sub-PolarSubpolar North Atlantic shift towardstoward smaller species under greenhouse warming that is not easily recovered even under CO₂ removal scenarios. Despite negative CO₂ emissions, the persistent collapse of larger-celled diatom populations and the shift toward smaller phytoplankton communities is a consequence of lower surface nutrient availability followed byfollowing the slowdown of the Atlantic Meridional Overturning Circulation (AMOC). This weakening of AMOC and associated nutrient transport exhibitexhibits delayed recovery. Depleting nutrients disrupts trophic dynamics, by altering primary limiting nutrient components, contributing to the continued decrease in diatoms and an increase in smaller phytoplankton. Consequently, the downsizing of the phytoplankton community indicates a large reduction in the ocean's

Introduction

The increase in anthropogenic carbon dioxide (CO₂) emissions is warming our planet. This poses a threat to nature, human beings, terrestrial and marine ecosystems, and climate systems, making global transnational efforts crucial to reduce additional carbon emissions (Cui et al., 2024; Gattuso et al., 2015; Nagelkerken and Connell, 2015). To do this, world leaders pledged in the 2015 Paris Agreement to limit longterm temperature increases to below 2°C, or ideally 1.5°C. Therefore, climate mitigation strategies, including negative CO₂ emissions through the development of Carbon Dioxide Removal (CDR) techniques, are necessary to curb global warming (Gasser et al., 2015; Meinshausen et al., 2009; Rogelj et al., 2016; Tong et al., 2019; Van Vuuren et al., 2018). However, the Earth's climate system may not be fully recovered, even if external forcing returns to baseline conditions, known as climate irreversibility. Numerous studies have reported that several physical variables have irreversible changes on a global &and regional scale, including temperature, precipitation, and ocean circulation under negative CO₂ emissions (An et al., 2022; Boucher et al., 2012; Hawkins et al., 2011; Jeltsch-Thömmes et al., 2020; Kim et al., 2024, 2022; Kug et al., 2022; Liu et al., 2023; Oh et al., 2024; Pathirana et al., 2023; Song et al., 2022). Irreversible changes in biological aspects have also been documented in both marine and terrestrial ecosystems, such as vegetation, wildfires, permafrost, primary productivity, and the carbon cycle (John et al., 2015; Park et al., 2025; Park and Kug, 2022; Schwinger and Tjiputra, 2018). Despite the wealth of research on climate irreversibility, few studies have focused on changes in phytoplankton communities, which play a crucial role in the global carbon cycle.

Marine phytoplankton form the foundation of ocean ecosystems (Platt et al., 2003; Richardson and Schoeman, 2004), mediate biogeochemical processes, and regulate climate (Behrenfeld et al., 2006; Field et al., 1998; Passow and Carlson, 2012). They are responsible for nearly half of the global primary production (PP; Field et al., 1998; Falkowski et al., 1998; Behrenfeld et al., 2006). Phytoplankton are vulnerable to climate change due to their sensitivity to external environmental conditions such as temperature (Anderson et al., 2021; Archibald et al., 2022; Behrenfeld et al., 2006; Doney, 2006), insolation (Marinov et al., 2010), and nutrient availability (Moore et al., 2013). Responses to external forcing vary among phytoplankton species, so the compositions of the phytoplankton community can influence their roles in food web organization and biogeochemical processes. Therefore, shifts in phytoplankton communities play a key role in various aspects, comparable to changes in their biomass (Barton et al., 2016; Winder and Sommer, 2012), and have significant socio-economic implications for fisheries and higher ecosystem levels. Conversely, changes in these aspects can also impact phytoplankton communities (Platt et al., 2003; Reid et al., 2000).

Previous studies have argued for a trend towards smaller phytoplankton communities under warmer climates using model simulations and observation-based research (Cael et al., 2021; Doney, 2006; Henson et al., 2021; Morán et al., 2010; Winder and Sommer, 2012). This downsizing of phytoplankton communities is likely to persist even under negative CO₂ emissions due to the irreversible responses of physical factors predicted under carbon mitigation scenarios. As smaller phytoplankton species dominate over larger cell-sized phytoplankton, photosynthesis becomes less efficient, and the gravitational sinking of particulate organic carbon (POC) in the

oceans weakens, reducing the amount of carbon sequestered over time (Boyd and Trull, 2007; Guidi et al., 2009; Maranon, 2014).

The Subpolar North Atlantic (SPNA)—Ocean is not only a critical region for climate change but also plays a vital role in the biological processes that govern CO₂ gas exchange between the air and seas (Bennington et al., 2009; Manabe and Stouffer, 1995; Sabine et al., 2004). Under global warming scenarios, there is a counterintuitive decrease in temperature in this region, resulting from the weakening of the Atlantic Meridional Overturning Circulation (AMOC), which drives deep convection in the SPNA region (Caesar et al., 2018; Liu et al., 2020; Oh et al., 2022). The weakening of the AMOC under global warming impairs volume transport from low to high latitudes, accompanied by decreases in nutrient-rich water conveyance (Schmittner, 2005). The SPNA region is one of the most significant areas for carbon uptake in the current regional climate and carbon cycle (Sabine et al., 2004). Nutrient deficiencies in the SPNA region potentially lead to shifts in plankton composition, resulting in large decreases in export production (EP) and net primary productivity (NPP) under future climate conditions. Previous studies have examined decreases in marine productivity in the SPNA under global warming (Moore et al., 2013; Schmittner, 2005; Steinacher et al., 2010). Despite the irreversibility of AMOC strength revealed by other studies, the irreversible responses of phytoplankton communities in this region have not been thoroughly explored.

Here, we aim to examine phytoplankton community shifts under negative CO₂ emissions and their implications as biological climate regulators. First, we analyze idealized CO₂ emission-driven simulations based on the Community Earth System Model 2 (CESM2) with multiple ensembles. The simulations incorporate biogeochemical processes coupled with a biogeochemistry model, and itexplicitly simulate three explicit phytoplankton functional types (PFTs): diatoms, small phytoplankton, and diazotrophs, each with distinct sourcesink parameters (See Methods for details). In the following sections, we report irreversible shifts in phytoplankton communities in the SPNA region and examine the mechanisms driving these results.

Methods

Bray Curtis dissimilarity

We quantified shifts in phytoplankton community using the Bray-Curtis (BC) dissimilarity metric frequently utilized in ecology and biology to quantify differences in species composition between two sites (Bray et al., 1957; Herren and McMahon, 2017). For two time periods, t_{\perp} and t_{\perp} , BC index is defined as below:

where, B_{ϵ}^{i} is the period-mean biomass of phytoplankton functional type (PFT) i, and R is the number of PFTs (here R = 3). BC ranges from 0 (identical composition) to 1 (no shared composition among PFTs). We computed BC index at each grid point using period mean PFT biomasses between the Climatology (2001–2011; t_i), and CO₂-down (2192–2202; t_2) periods.

Model Configuration

In this study, we employed Community Earth System Model version 2 (CESM2)In this study, we employed Community Earth System Model version 2 (CESM2; Danabasoglu et al., 2020) to investigate marine biogeochemical cycles, focusing on the dynamics of the nutrient and phytoplankton communities in the Southern Ocean (SO). SPNA region. The marine ecosystem within CESM2 is represented by the Marine Biogeochemical Library (MARBL), which incorporates three explicitly modeled phytoplankton functional groups—diatoms, diazotroph, pico/nano (small) phytoplankton—as well as one implicit group (calcifiers) and a single zooplankton group, each with distinct source-sink parameters. MARBL also simulates 32 different tracers, which include 17 abiotic constituents such as dissolved inorganic and organic carbon, alkalinity, nutrients, and oxygen, along with 15 biotic tracers associated with phytoplankton biomass (e.g., Carbon (C), Phosphorus (P), Nitrogen (N), Silica (Si), Iron (Fe), and Calcium Carbonate (CaCO₃)), as well as zooplankton carbon.

Within MARBL, phytoplankton growth rates depend on multiple environmental parameters, including temperature, nutrient limitation, and light availability, as detailed in Long et al (2021). Nutrient limitation is determined by Liebig's law of the minimum, whereby the nutrient available in the smallest quantities limits phytoplankton growth. Changes in PFT concentrations are calculated by source (i.e., net primary productivity) and sink (grazing, linear mortality, and aggregation) terms as elaborated in Long et al (2021).

Long et al (2021) evaluated the model's performance in simulating biogeochemical variables such as macronutrient (Nitrate; NO₃, Phosphate; PO₄, Silicate; SiO₃) distribution and NPP and export production (EP). They showed that MARBL effectively simulates the geographical patterns of macronutrients in the SPNA region compared to World Ocean Atlas (WOA) observations. Moreover, comparisons with satellite observations revealed that the global distribution of NPP simulated by MARBL exhibits similar patterns, albeit with slight differences

in magnitude.

Experimental Design

We analyzed an idealized negative CO₂ emissions pathway that effectively reduces emissions incrementally, considering the development of Carbon Dioxide Removal (CDR) technology and global mitigation efforts. In our experiments, anthropogenic CO₂ emissions increase linearly from an initial CO₂ concentration of 383 ppm to the year 2050, based on the SSP5-8.5 scenario. (Fig. S1), as same as used in Park et al (2025). Subsequently, emissions decrease at the same rate until the global mean atmospheric CO₂ concentration returns to its original value (in the year 2196). Immediately after reaching this level, net-zero emissions are maintained until the end of the simulation (year 2400). The atmospheric CO₂ level peaks in the year 2107 (725 ppm), just a few years before achieving net-zero emissionsemission. For better readability, we define periods as follows: CO₂ increasing period (2001-2107) and CO₂ decreasing period (2108-2196), and restoring period as the duration of net-zero emission (2197-2400), respectively. We also have defined the first 11 years (2001-2011) as the "Climatology period", and the 11 years (2192-2202) at the end of the CO₂ decreasing period as the "CO₂ down period" to identify irreversible changes of climatic variables under the same CO₂ conditions. We have run a total of ten ensemble members, each with slightly different initial conditions, to consider the variability.

Bray-Curtis dissimilarity

We quantified shifts in phytoplankton community using the Bray-Curtis (BC) dissimilarity metric frequently utilized in ecology and biology to quantify differences in species composition between two sites (Bray et al., 1957; Herren and McMahon, 2017). For two time periods, t_L and t_2 , the BC index is defined as below:

140 Bray-Curtis (BC) index = 1
$$-\frac{2\sum_{i=1}^{R} \min (B_{t_1}^i, B_{t_2}^i)}{\sum_{i=1}^{R} (B_{t_1}^i + B_{t_2}^i)}$$
 (1)

where, B_t^i is the period-mean biomass of phytoplankton functional type (PFT) i, and R is the number of PFTs (here R = 3). BC ranges from 0 (identical composition) to 1 (no shared composition among PFTs). We computed the BC index at each grid point using period-mean PFT biomasses between the Climatology (2001-2011; t_I), and CO₂-down (2192-2202; t_I) periods.

Results

Irreversible phytoplankton community shifts to CO2 forcing in SPNA region

We investigate the shifts in phytoplankton communities between the climatology period and the CO₂ down period. The statistical method known as BC dissimilarity was used to examine the similarity of the phytoplankton communities between the two periods following Cael et al (2021; Detail in Methods). There are pronounced positive values (indicating less similarity) of dissimilarity at high latitudes in the northern hemisphere (NH), including the Arctic and SPNA region. Notably, the most significant shifts in phytoplankton communities emerge in the SPNA region, indicating substantial variations in phytoplankton composition (Fig. 1a).

Fig. 1b presents a time series of area-averaged PFT biomass in the SPNA region. As atmospheric CO₂ concentrations increase, diatoms and small phytoplankton exhibit a significant decrease and increase, respectively. These results are consistent with previous studies, which have reported shifts towards smaller PFT-dominant phytoplankton communities in a warmer world (Cael et al., 2021; Doney, 2006; Henson et al., 2021; Morán et al., 2010; Winder and Sommer, 2012). These variations in PFT biomass persist under negative CO₂ emissions. While small phytoplankton increase over time and has a peak in the middle of the CO₂ decreasing period, diatoms continue to decrease and have a minimum value at the same time. Similarly, the diazotroph concentrations decrease, except for a slight initial increase, eventually reaching a minimum at the end of the CO₂ decreasing period. During the restoring period, all PFTs—except diazotrophs, which overshoot—return to near their initial values with diatom concentrations showing a slight weakening. Comparing the two periods (CO₂ down - Climatology) with the same atmospheric CO₂ concentration reveals substantial shifts in the phytoplankton community. Specifically, there is a large decrease in larger cell-sized phytoplankton and an increase in smaller cell-sized phytoplankton, indicating significant downsizing of the phytoplankton community.

All PFTs exhibit strong irreversible shifts in response to CO₂ forcing (Figs. 1c-e). In particular, diatom concentrations decreased to 24% of their initial value during the CO₂ increasing period, while small phytoplankton increased by about 283% compared to the Climatology period. The phytoplankton biomass remained nearly constant during the CO₂ decreasing period when the atmospheric CO₂ concentration returned to its initial value of 383 ppm. These results indicate shifts in the phytoplankton community towards dominance by smaller phytoplankton in the SPNA region, despite the same atmospheric CO₂ concentration. In addition, although the diazotroph concentrations constitute a relatively smaller portion of the total PFTs, their pronounced decline during the CO₂ decreasing period leads to a weakening of biological N fixation to the ocean (Fig. S1aS2a). The diazotrophs show different behavior compared to the other two species because of their temperature-limited biological properties (Breitbarth et al., 2007; Yi et al., 2020). Consequently, temporal changes in Sea Surface Temperature (SST), diazotroph concentrations, and N fixation rates in the SPNA region are all closely aligned (Fig. S1S2).

Smaller phytoplankton have greater competitiveness in oligotrophic and stratified marine environments in a warmer world due to their enhanced surface area-to-volume ratio (Morán et al., 2010; Winder and Sommer,

2012). Within MARBL—the biogeochemical component of the CESM2 Earth System Model—the advantage of smaller phytoplankton in low-nutrient environments is represented by prescribing different constant half-saturation coefficients for each PFT, reflecting the observed differences among phytoplankton size classes in the real ocean (Long et al., 2021). For instance, two PFTs (diatom and small phytoplankton) may possess the same maximum growth rate; however, the half-saturation coefficient is parameterized to be smaller for small phytoplankton. This implies that small phytoplankton can achieve their maximum growth rate with a lower nutrient concentration. Furthermore, the decrease in diatoms due to the shift towards oligotrophic conditions may lead to a reduction in zooplankton and a weakening of grazing by higher-level predators, thereby promoting the growth of phytoplankton. The time series of source and sink terms integrated to 100 m depth exhibits that grazing is the dominant sink contribution to loss for both PFTs, with other terms having relatively minor effects (Fig. \$22S3).

Irreversibility of AMOC strength and shift in the primary nutrient limiting component.

The spatial distribution of PFT biomass differences between the two periods reveals a significant shift across the SPNA (Figs. 2a-c). Across the entire Atlantic and Arctic regions, and even globally (not shown), the most dramatic differences are observed in the SPNA region. For diazotrophs, whose growth rates are temperature-dependent, high latitudes above 50°N exhibit scant biomass climatologically and no variations (Fig. \$3\$4, Fig. 2c). Except for diazotrophs, changes in phytoplankton concentrations are generally driven by nutrient availability. While NO₃ is commonly considered the most limiting nutrient globally, observation-based studies have identified silicate as the primary limiting component for phytoplankton growth in the SPNA region (Allen et al., 2005). The CESM2 biogeochemical model, MARBL, also well-simulates well the Si-limited growth of diatoms in the SPNA region, consistent with observations (Long et al., 2021). The spatial distribution of differences between the two periods for both macronutrients (NO₃, SiO₃) shows similar patterns to PFT biomass changes.

The North Atlantic, including the SPNA region, is characterized by deep convection associated with the AMOC. Changes in the AMOC lead to significant physical alterations in the SPNA region. In particular, the AMOC plays a pivotal role in transporting water volumes from low to high latitudes, and through this process, nutrient-rich water transport can trigger biological changes (Boot et al., 2023). Under global warming, AMOC is expected to progressively weaken due to increased surface temperature and the influx of freshwater. Additionally, it has been reported that under negative emissions, AMOC strength will not recover immediately but will instead decrease further with a delay (An et al., 2021; Oh et al., 2022). This implies that changes in AMOC strength may influence shifts in the phytoplankton community in the SPNA region under a climate mitigation scenario.

Thus, we investigate the changes in AMOC strength and nutrient concentrations in our simulations (Fig. 3a). In our experiments, the intensity of the AMOC continues to decrease with increasing atmospheric CO₂ concentration, persisting until the middle of the CO₂ mitigation pathway and reaching its weakest state around the year 2142 (Fig. 3a). Subsequently, the AMOC gradually strengthens again, returning to its initial condition with

overshooting during the restoring period (An et al., 2021; Jackson et al., 2014; Wu et al., 2011). Consistent with the weakening of AMOC strength over time, both nutrient concentrations also continue to decline (Fig. 3a). Interestingly, while both nutrients decline over time, the reduction in SiO₃ concentration halts around the year 2075 and remains steady until approximately the year 2250 before recovering. Conversely, NO₃ decreases until around the year 2170, past the point of minimal AMOC strength, and then recovers with the AMOC turnabout. The distinct responses of SiO₃ and NO₃ to CO₂ forcing arise largely due to the diverging responses of PFTs from the climatology period to the CO₂ down period. While decreases in diatoms-driven NPP reduce the consumption rates of both SiO₃ and NO₃, increases in small-phytoplankton-driven NPP counterbalance the decreasing NO₃ consumption rates, resulting in a more persistent decline in NO₃ (Fig. S6S7). Reduced diazotrophs-driven NPP and associated N-fixation also contribute to further decline in surface NO₃ concentrations. Changes in the limiting nutrient components may affect the nutrient dynamics of phytoplankton, particularly diatoms, which are composed of larger cells in the SPNA region.

We identified changes in the limiting nutrients for the growth of two PFTs (diatom, small phytoplankton). The spatial patterns of limiting nutrients are shown in FigFigs. 3c and 3d for diatoms and in Fig. S4e and Fig. S4dFigs. S5b-c for small phytoplankton, with the SPNA-averaged time series are shown in Fig. 3b and Fig. S4aS5a. When spatially averaged, small phytoplankton, unaffected by SiO₃ availability, experience N limitation throughout all timeframes owing to continuously decreasing NO₃ levels (Fig. S4S5). For diatoms, however, the predominant limiting nutrient shifts from Silicon (Si) to N around the year 2076, coinciding with the stabilization of SiO₃ levels (Figs. 3a-b). During the Climatology period, Si limitation for diatoms diatom dominates across most of the SPNA region (Fig. 3c). However, as NO₃ decreases more rapidly than SiO₃, N limitation spreads across the SNPA region, eventually overtaking Si limitation. By the CO₂ down period, Si limitation becomes confined only to small regions, with most areas transitioning to N limitation. (Figs. 3c-d).

From the Irminger Sea, located beneath Greenland, to the Nordic Sea, the Si-limited environment persists even during the CO₂ down period. This region, characterized by intense deep convection in the present climate (Heuzé, 2017; Renssen et al., 2005), exhibits the most pronounced shallowing of the mixed layer depth (MLD) than elsewhere, indicating that it is particularly affected by the weakening of the AMOC (Fig. S5). Consequently, SiO₃ concentrations are significantly reduced compared to other regions, maintaining Si limitation. Furthermore, even as the AMOC enters a recovery phase, nutrient levels do not rebound immediately and exhibit a delayed response. S6). Consequently, SiO₃ concentrations are significantly reduced compared to other regions, maintaining Si limitation. Furthermore, even as the AMOC enters a recovery phase, nutrient levels do not rebound immediately and exhibit a delayed response. During the weakened AMOC phase, MLD in the SPNA region remains in a shutdown state, and its recovery requires sufficient salt-advection accompanying AMOC strengthening (Oh et al., 2022). Therefore, the MLD can begin to recover after the salt advection has sufficiently accumulated. In addition, global warming strengthens Southern Ocean (SO) productivity, which weakens global nutrient redistribution—intensifying deep-ocean nutrient trapping and reducing surface nutrients that might persist even under climate mitigation (Moore et al., 2018; Laufkötter and Gruber, 2018). Therefore, even when the AMOC starts to recover, the amount of nutrients transported from the Southern Hemisphere and low latitudes

remains reduced compared to the climatology period. As a result, the recovered nutrient levels stay below the climatological state, giving rise to the delayed recovery. Thus, lagged nutrient retrieval causes a corresponding lagged response in phytoplankton community recovery. As the AMOC strength and nutrient transport are reinstated, nutrient concentrations increase sufficiently by around the year 2250, causing a return to Si limitation. This suggests that while the AMOC plays a critical role in nutrient distribution and the marine ecosystem in the SPNA region, the phytoplankton community may experience stronger irreversible changes than the recovery of AMOC strength under a climate mitigation scenario.

Implication of phytoplankton community shift on POC export

The shift towards smaller phytoplankton communities can have significant ecological, biogeochemical, and climatic impacts. Phytoplankton, composed of larger cells, possess a greater capacity for sequestering CO2 through photosynthesis and gravitational sinking into the ocean. In contrast, organic carbon exported by smaller phytoplankton is more readily degraded by higher-level predators such as bacteria and zooplankton, and can be re-released back to the water column as CO₂ quickly compared to diatoms (Leblanc et al., 2018; Tréguer et al., 2018). Therefore, the collapse of diatom populations during the CO₂ down periods could lead to a loss of biological carbon sequestration competence (biological pump). This attenuation is particularly evident in the SPNA region, where the phytoplankton community shifts are most pronounced (Fig. 4a). The weakening of the biological pump is evident throughout the SNPASPNA region and extends beyond in parts of the Arctic region. Consistent with the strong biological irreversible responses observed in the above results, there is a significant irreversible decline in the organisms' ability to export carbon (POC flux). The abundance of diatoms, which typically dominate the biological carbon pump, has decreased to about a fourth, while small phytoplankton have increased by a factor of 2.7. As a result, when CO₂ concentrations return to initial levels, the POC flux is less than half of the initial condition, indicating that the decrease in diatoms plays a dominant role in POC export changes. Specifically, the SPNA region, currently a key area for CO₂ sequestration (Sabine et al., 2004), is projected to be less effective at exporting carbon than the global average after CO₂ mitigation (Figs 4b-c). Consequently, while the North Atlantic Ocean is presently known for its strong biological pump, it may lose this status under CO₂ mitigation scenarios (Fig. 4). Therefore, the longer climate mitigation is delayed, the more the miniaturization of phytoplankton communities will accelerate, further slowing down the marine biological pump.

Therefore, even if atmospheric CO₂ concentrations return to their original levels through negative emissions, marine ecosystems, especially the composition of PFTs will exhibit strong irreversible shifts. This disrupted phytoplankton community has the potential to impact regional &and global trophic dynamics and food webs, as well as commercial fisheries and more. Moreover, if global warming accelerates again in the context of a downsizing of the phytoplankton community, it is possible that we will experience even more abrupt climate change than at present, as the Earth's capacity for biological carbon export is diminished.

Discussion

This study conducts idealized CO₂ emission-driven simulations using multiple ensembles to investigate how phytoplankton communities respond under CO₂ mitigation scenarios. When atmospheric CO₂ concentration returns to initial levels through negative emissions, we observe the most significant changes in the composition of PFTs in the SPNA region (Fig. 1a). For example, smaller phytoplankton populations increase, and the concentrations of large cell-sized diatoms collapse (Figs. 1b-d). The diazotroph concentrations significantly decrease, primarily reflecting the response to oceanic temperature changes, while suppressed nutrient availability contributes as well (Fig. 1b, e, Fig. \$\frac{\$\mathbf{S}\mathbf{S}\mathbf{S}}{2}\). Across the SPNA region, macronutrients (NO₃, SiO₃) can substantially limit phytoplankton growth (Figs. 2d-e, Fig. 3a). As the globe warms, the AMOC gradually weakens and exhibits strong irreversible changes under negative CO₂ emissions. The reductions in nutrient concentrations are strongly correlated with AMOC weakening (Fig. 3a). The weakening of the AMOC leads to regional and global climatic variations, particularly affecting nutrient transport, which is essential for biological activities in the SPNA region. Furthermore, shifts in the phytoplankton community alter trophic dynamics, accelerating NO₃ depletion and creating an N-limited environment for diatom growth (Fig. 3b). The downsizing of the phytoplankton community is markedly slow to recover, even as AMOC strength rebounds, due to the delayed recovery of nutrient levels. Consequently, PFTs exhibit irreversible shifts, which could have significant biological, biogeochemical, and climatic implications. Carbon export capacity in the SPNA region is reduced by more than 50% compared to the present climate.

Our study reveals that global warming-driven irreversible changes in AMOC strength can trigger irreversibility not only in physical parameters, such as SST and salinity, but also in cascading biological and biogeochemical responses. Pronounced shifts in phytoplankton communities in the Subpolar North Atlantic involve negative feedback, resulting in the loss of biological carbon export capacity, which in turn exacerbates global warming. In other words, multiple stressors—physical, trophic, and biological—can interact and weaken the resilience of marine ecosystems and the biological carbon pump system (Conversi et al., 2015).

However, our study has several limitations and potential avenues for further research. Our study uses CO₂ emission-driven idealized experiments with ten ensembles but relies on a single model, CESM2, which could render the results model-dependent. It has been documented that CESM2 simulates AMOC weakening more sensitively than other Earth System Models (Needham et al., 2024; Schwinger et al., 2022), potentially leading to a propensity to overestimate marine ecosystem changes. However, the GFDL-ESM4 and CNRM-ESM2-1, as part of the CDRMIP experiments in CMIP6, include diatom variables and exhibit consistent weakening in diatom concentrations alongside AMOC weakening in the SPNA region (Fig. S7Figs. S8a-b). In GFDL-ESM4, diatom concentrations recover comparably after CO₂ is decreased to the initial level, yet the pathway during the CO₂ Ramp upramp-down period does not follow the same pathway as the CO₂ Rampramp-up period, (Fig. S8c), indicating hysteresisirreversibility in both GFDL-ESM4 and CNRM-ESM2-1. Another limitation of this study is that the CESM2 MARBL biogeochemical model includes only three PFTs—diatoms, small phytoplankton, and diazotrophs. While this study offers valuable insights into the broader shifts in phytoplankton community structure

under climate mitigation scenarios, it is essential to acknowledge the limitations of representing the complex phytoplankton community with only three PFTs. Analyzing changes in specific PFTs is beyond the scope of this study and requires further investigation of the simplicity/diversity of PFTs in simulating the global biogeochemical cycle. However, the model's simplicity is still advantageous in capturing future trends in phytoplankton as a function of their cell size and the underlying mechanisms driving phytoplankton dynamics and their biogeochemical implications. While the simplification of the CESM2 MARBL model to three PFTs could be considered a limitation, it does not diminish the significance of the results.

This study demonstrates that CESM effectively captures key trends in phytoplankton community shifts and their broader implications, providing a strong framework for assessing the impacts of climate change on marine ecosystems. This study advances our understanding of the potential trajectories of marine biogeochemical processes and their environmental and economic implications. Future research could further enhance these findings by incorporating a more diverse range of PFTs.

335	Data Availability Statement
336	The data used in this study will be available from https://doi.org/10.6084/m9.figshare.27058897 , and the CMIP6
337	archives are freely available from https://esgf-node.llnl. gov/projects/cmip6.
338	
339	Code availability
340	The computer codes that support the analysis within this paper are available from the corresponding author on
341	request.
342	
343	Acknowledgements
344	This work is supported by the Korea Meteorological Administration Research and Development Program under
345	Grant (RS-2025-02222417) and Korea Environment Industry & Technology Institute(KEITI) through Project for
346	developing an observation-based GHG emissions geospatial information map, funded by Korea Ministry of
347	Environment(MOE) (RS-2023-00232066). This work was supported by Institute of Information &
348	communications Technology Planning & Evaluation (IITP) grant funded by the Korea government(MSIT)
349	[NO.RS-2021-II211343, Artificial Intelligence Graduate School Program (Seoul National University)]. This work
350	was supported by the National Supercomputing Center with supercomputing resources associated with technical
351	support (KSC-2025-CHA-0001) and the National Center for Meteorological Supercomputer of the Korea
352	Meteorological Administration (KMA) and the Korea Research Environment Open NETwork (KREONET),
353	respectively
354	
355	Competing interests
356	The authors declare no competing interests.

12

357

358

Author contributions

D.-G. Lee compiled the data, conducted analyses, prepared the figures, and wrote the manuscript. J.-S. Kug designed the research and wrote the majority of the manuscript content. All the authors discussed the study results and reviewed the manuscript.

359

360

- 362 Reference
- Allen, J. T., Brown, L., Sanders, R., Moore, C. M., Mustard, A., Fielding, S., Lucas, M., Rixen, M., Savidge, G.,
- Henson, S., and Mayor, D.: Diatom carbon export enhanced by silicate upwelling in the northeast Atlantic, Nature,
- 365 437, 728–732, https://doi.org/10.1038/nature03948, 2005.
- An, S. Il, Shin, J., Yeh, S. W., Son, S. W., Kug, J. S., Min, S. K., and Kim, H. J.: Global Cooling Hiatus Driven
- 367 by an AMOC Overshoot in a Carbon Dioxide Removal Scenario, Earth's Futur., 9,
- 368 https://doi.org/10.1029/2021EF002165, 2021.
- An, S. Il, Park, H. J., Kim, S. K., Shin, J., Yeh, S. W., and Kug, J. S.: Intensity changes of Indian Ocean dipole
- mode in a carbon dioxide removal scenario, npj Clim. Atmos. Sci., 5, 1–8, https://doi.org/10.1038/s41612-022-
- 371 00246-6, 2022.
- Anderson, S. I., Barton, A. D., Clayton, S., Dutkiewicz, S., and Rynearson, T. A.: Marine phytoplankton
- 373 functional types exhibit diverse responses to thermal change, Nat. Commun., 12, 1-9
- 374 https://doi.org/10.1038/s41467-021-26651-8, 2021.
- 375 Archibald, K. M., Dutkiewicz, S., Laufkötter, C., and Moeller, H. V.: Thermal Responses in Global Marine
- Planktonic Food Webs Are Mediated by Temperature Effects on Metabolism, J. Geophys. Res. Ocean., 127, 1–
- 377 18, https://doi.org/10.1029/2022JC018932, 2022.
- Barton, A. D., Irwin, A. J., Finkel, Z. V., and Stock, C. A.: Anthropogenic climate change drives shift and shuffle
- in North Atlantic phytoplankton communities, Proc. Natl. Acad. Sci. U. S. A., 113, 2964-2969,
- 380 https://doi.org/10.1073/pnas.1519080113, 2016.
- Behrenfeld, M. J., O'Malley, R. T., Siegel, D. A., McClain, C. R., Sarmiento, J. L., Feldman, G. C., Milligan, A.
- J., Falkowski, P. G., Letelier, R. M., and Boss, E. S.: Climate-driven trends in contemporary ocean productivity,
- Nature, 444, 752–755, https://doi.org/10.1038/nature05317, 2006.
- Bennington, V., McKinley, G. A., Dutkiewicz, S., and Ullman, D.: What does chlorophyll variability tell us about
- export and air-sea CO 2 flux variability in the North Atlantic?, Global Biogeochem. Cycles, 23, 1–11,
- 386 https://doi.org/10.1029/2008GB003241, 2009.

- Boot, A., von der Heydt, A. S., and Dijkstra, H. A.: Effect of Plankton Composition Shifts in the North Atlantic
- on Atmospheric pCO2, Geophys. Res. Lett., 50, https://doi.org/10.1029/2022GL100230, 2023.
- Boucher, O., Halloran, P. R., Burke, E. J., Doutriaux-Boucher, M., Jones, C. D., Lowe, J., Ringer, M. A.,
- Robertson, E., and Wu, P.: Reversibility in an Earth System model in response to CO2 concentration changes,
- 391 Environ. Res. Lett., 7, https://doi.org/10.1088/1748-9326/7/2/024013, 2012.
- Boyd, P. W. and Trull, T. W.: Understanding the export of biogenic particles in oceanic waters: Is there consensus?,
- 393 Prog. Oceanogr., 72, 276–312, https://doi.org/10.1016/j.pocean.2006.10.007, 2007.
- Bray, J. R., Curtis, J. T., and Roger, J.: This content downloaded from 147.8.31.43 on Mon, Source Ecol. Monogr.,
- 395 27, 325–349, 1957.
- 396 Breitbarth, E., Oschlies, A., and LaRoche, J.: Physiological constraints on the global distribution of
- 397 Trichodesmium Effect of temperature on diazotrophy, Biogeosciences, 4, 53–61, https://doi.org/10.5194/bg-4-
- 398 53-2007, 2007.
- Cael, B. B., Dutkiewicz, S., and Henson, S.: Abrupt shifts in 21st-century plankton communities, Sci. Adv., 7,
- 400 https://doi.org/10.1126/sciadv.abf8593, 2021.
- 401 Caesar, L., Rahmstorf, S., Robinson, A., Feulner, G., and Saba, V.: Observed fingerprint of a weakening Atlantic
- 402 Ocean overturning circulation, Nature, 556, 191–196, https://doi.org/10.1038/s41586-018-0006-5, 2018.
- Conversi, A., Dakos, V., Gårdmark, A., Ling, S., Folke, C., Mumby, P. J., Greene, C., Edwards, M., Blenckner,
- T., Casini, M., Pershing, A., and Möllmann, C.: A Holistic view of Marine Regime shifts, Philos. Trans. R. Soc.
- 405 B Biol. Sci., 370, 1–8, https://doi.org/10.1098/rstb.2013.0279, 2015.
- 406 Cui, J., Zheng, M., Bian, Z., Pan, N., Tian, H., Zhang, X., Qiu, Z., Xu, J., and Gu, B.: Elevated CO2 levels promote
- 407 both carbon and nitrogen cycling in global forests, Nat. Clim. Chang., 14, 511-517,
- 408 https://doi.org/10.1038/s41558-024-01973-9, 2024.
- Danabasoglu, G., Lamarque, J. F., Bacmeister, J., Bailey, D. A., DuVivier, A. K., Edwards, J., Emmons, L. K.,
- 410 Fasullo, J., Garcia, R., Gettelman, A., Hannay, C., Holland, M. M., Large, W. G., Lauritzen, P. H., Lawrence, D.
- 411 M., Lenaerts, J. T. M., Lindsay, K., Lipscomb, W. H., Mills, M. J., Neale, R., Oleson, K. W., Otto-Bliesner, B.,

- Phillips, A. S., Sacks, W., Tilmes, S., van Kampenhout, L., Vertenstein, M., Bertini, A., Dennis, J., Deser, C.,
- 413 Fischer, C., Fox-Kemper, B., Kay, J. E., Kinnison, D., Kushner, P. J., Larson, V. E., Long, M. C., Mickelson, S.,
- 414 Moore, J. K., Nienhouse, E., Polvani, L., Rasch, P. J., and Strand, W. G.: The Community Earth System Model
- 415 Version 2 (CESM2), J. Adv. Model. Earth Syst., 12, 1–35, https://doi.org/10.1029/2019MS001916, 2020.
- Doney, S. C.: Plankton in a warmer world, Nature, 444, 695–696, https://doi.org/10.1038/444695a, 2006.
- 417 Falkowski, P. G., Barber, R. T., and Smetacek, V.: Biogeochemical controls and feedbacks on ocean primary
- 418 production, Science (80-.)., 281, 200–206, https://doi.org/10.1126/science.281.5374.200, 1998.
- 419 Field, C. B., Behrenfeld, M. J., Randerson, J. T., and Falkowski, P.: Primary production of the biosphere:
- 420 Integrating terrestrial and oceanic components, Science (80-.)., 281, 237-240,
- 421 https://doi.org/10.1126/science.281.5374.237, 1998.
- 422 Gasser, T., Guivarch, C., Tachiiri, K., Jones, C. D., and Ciais, P.: Negative emissions physically needed to keep
- 423 global warming below 2°C, Nat. Commun., 6, https://doi.org/10.1038/ncomms8958, 2015.
- 424 Gattuso, J. P., Magnan, A., Billé, R., Cheung, W. W. L., Howes, E. L., Joos, F., Allemand, D., Bopp, L., Cooley,
- S. R., Eakin, C. M., Hoegh-Guldberg, O., Kelly, R. P., Pörtner, H. O., Rogers, A. D., Baxter, J. M., Laffoley, D.,
- Osborn, D., Rankovic, A., Rochette, J., Sumaila, U. R., Treyer, S., and Turley, C.: Contrasting futures for ocean
- 427 and society from different anthropogenic CO2 emissions scenarios, Science (80-.)., 349,
- 428 https://doi.org/10.1126/science.aac4722, 2015.
- 429 Guidi, L., Stemmann, L., Jackson, G. A., Ibanez, F., Claustre, H., Legendre, L., Picheral, M., and Gorsky, G.:
- 430 Effects of phytoplankton community on production, size and export of large aggregates: A world-ocean analysis,
- 431 Limnol. Oceanogr., 54, 1951–1963, https://doi.org/10.4319/lo.2009.54.6.1951, 2009.
- Hawkins, E., Smith, R. S., Allison, L. C., Gregory, J. M., Woollings, T. J., Pohlmann, H., and De Cuevas, B.:
- 433 Bistability of the Atlantic overturning circulation in a global climate model and links to ocean freshwater transport,
- 434 Geophys. Res. Lett., 38, 1–6, https://doi.org/10.1029/2011GL047208, 2011.
- Henson, S. A., Cael, B. B., Allen, S. R., and Dutkiewicz, S.: Future phytoplankton diversity in a changing climate,
- 436 Nat. Commun., 12, 1–8, https://doi.org/10.1038/s41467-021-25699-w, 2021.

- 437 Herren, C. M. and McMahon, K. D.: Cohesion: A method for quantifying the connectivity of microbial
- 438 communities, ISME J., 11, 2426–2438, https://doi.org/10.1038/ismej.2017.91, 2017.
- 439 Heuzé, C.: North Atlantic deep water formation and AMOC in CMIP5 models, Ocean Sci., 13, 609-622,
- 440 https://doi.org/10.5194/os-13-609-2017, 2017.
- Jackson, L. C., Schaller, N., Smith, R. S., Palmer, M. D., and Vellinga, M.: Response of the Atlantic meridional
- 442 overturning circulation to a reversal of greenhouse gas increases, Clim. Dyn., 42, 3323-3336,
- 443 https://doi.org/10.1007/s00382-013-1842-5, 2014.
- Jeltsch-Thömmes, A., Stocker, T. F., and Joos, F.: Hysteresis of the Earth system under positive and negative
- 445 CO2emissions, Environ. Res. Lett., 15, https://doi.org/10.1088/1748-9326/abc4af, 2020.
- John, J. G., Stock, C. A., and Dunne, J. P.: A more productive, but different, ocean after mitigation, Geophys. Res.
- 447 Lett., 42, 9836–9845, https://doi.org/10.1002/2015GL066160, 2015.
- 448 Keith Moore, J., Fu, W., Primeau, F., Britten, G. L., Lindsay, K., Long, M., Doney, S. C., Mahowald, N., Hoffman,
- 449 F., and Randerson, J. T.: Sustained climate warming drives declining marine biological productivity, Science
- 450 (80-.)., 359, 113–1143, https://doi.org/10.1126/science.aao6379, 2018.
- 451 Kim, G. Il, Oh, J. H., Shin, N. Y., An, S. Il, Yeh, S. W., Shin, J., and Kug, J. S.: Deep ocean warming-induced El
- 452 Niño changes, Nat. Commun., 15, 1–8, https://doi.org/10.1038/s41467-024-50663-9, 2024.
- Kim, S. K., Shin, J., An, S. Il, Kim, H. J., Im, N., Xie, S. P., Kug, J. S., and Yeh, S. W.: Widespread irreversible
- 454 changes in surface temperature and precipitation in response to CO2 forcing, Nat. Clim. Chang., 12,
- 455 https://doi.org/10.1038/s41558-022-01452-z, 2022.
- 456 Kug, J. S., Oh, J. H., An, S. Il, Yeh, S. W., Min, S. K., Son, S. W., Kam, J., Ham, Y. G., and Shin, J.: Hysteresis
- 457 of the intertropical convergence zone to CO2 forcing, Nat. Clim. Chang., 12, 47-53,
- 458 https://doi.org/10.1038/s41558-021-01211-6, 2022.
- 459 Laufkötter, C. and Gruber, N.: Will marine productivity wane?, Science (80-.)., 359, 1103-1104,
- 460 <u>https://doi.org/10.1126/science.aat0795, 2018.</u>
- 461 Leblanc, K., Quéguiner, B., Diaz, F., Cornet, V., Michel-Rodriguez, M., Durrieu De Madron, X., Bowler, C.,

- 462 Malviya, S., Thyssen, M., Grégori, G., Rembauville, M., Grosso, O., Poulain, J., De Vargas, C., Pujo-Pay, M.,
- and Conan, P.: Nanoplanktonic diatoms are globally overlooked but play a role in spring blooms and carbon
- 464 export, Nat. Commun., 9, 1–12, https://doi.org/10.1038/s41467-018-03376-9, 2018.
- 465 Liu, C., An, S. Il, Jin, F. F., Stuecker, M. F., Zhang, W., Kug, J. S., Yuan, X., Shin, J., Xue, A., Geng, X., and
- 466 Kim, S. K.: ENSO skewness hysteresis and associated changes in strong El Niño under a CO2 removal scenario,
- 467 npj Clim. Atmos. Sci., 6, https://doi.org/10.1038/s41612-023-00448-6, 2023.
- Liu, W., Fedorov, A. V., Xie, S. P., and Hu, S.: Climate impacts of a weakened Atlantic meridional overturning
- circulation in a warming climate, Sci. Adv., 6, 1–8, https://doi.org/10.1126/sciadv.aaz4876, 2020.
- 470 Long, M. C., Moore, J. K., Lindsay, K., Levy, M., Doney, S. C., Luo, J. Y., Krumhardt, K. M., Letscher, R. T.,
- 471 Grover, M., and Sylvester, Z. T.: Simulations With the Marine Biogeochemistry Library (MARBL), J. Adv. Model.
- 472 Earth Syst., 13, https://doi.org/10.1029/2021MS002647, 2021.
- 473 Manabe, S. and Stouffer, R. B.: Freshwater input to the North Atlantic Ocean, Nature, 378, 165–167, 1995.
- 474 Maranon, E.: Cell Size as a Key Determinant of Phytoplankton Metabolism and Community Structure, Ann. Rev.
- 475 Mar. Sci., 7, 241–264, https://doi.org/10.1146/annurev-marine-010814-015955, 2014.
- 476 Marinov, I., Doney, S. C., and Lima, I. D.: Response of ocean phytoplankton community structure to climate
- change over the 21st century: Partitioning the effects of nutrients, temperature and light, Biogeosciences, 7, 3941–
- 478 3959, https://doi.org/10.5194/bg-7-3941-2010, 2010.
- Meinshausen, M., Meinshausen, N., Hare, W., Raper, S. C. B., Frieler, K., Knutti, R., Frame, D. J., and Allen, M.
- 480 R.: Greenhouse-gas emission targets for limiting global warming to 2°C, Nature, 458, 1158–1162,
- 481 https://doi.org/10.1038/nature08017, 2009.
- 482 Moore, C. M., Mills, M. M., Arrigo, K. R., Berman-Frank, I., Bopp, L., Boyd, P. W., Galbraith, E. D., Geider, R.
- 483 J., Guieu, C., Jaccard, S. L., Jickells, T. D., La Roche, J., Lenton, T. M., Mahowald, N. M., Marañón, E., Marinov,
- 484 I., Moore, J. K., Nakatsuka, T., Oschlies, A., Saito, M. A., Thingstad, T. F., Tsuda, A., and Ulloa, O.: Processes
- and patterns of oceanic nutrient limitation, Nat. Geosci., 6, 701–710, https://doi.org/10.1038/ngeo1765, 2013.
- 486 Morán, X. A. G., López-Urrutia, Á., Calvo-Díaz, A., and LI, W. K. W.: Increasing importance of small

- 487 phytoplankton in a warmer ocean, Glob. Chang. Biol., 16, 1137-1144, https://doi.org/10.1111/j.1365-
- 488 2486.2009.01960.x, 2010.
- 489 Nagelkerken, I. and Connell, S. D.: Global alteration of ocean ecosystem functioning due to increasing human
- 490 CO2 emissions, Proc. Natl. Acad. Sci. U. S. A., 112, 13272–13277, https://doi.org/10.1073/pnas.1510856112,
- 491 2015.
- 492 Needham, M. R., Falter, D. D., and Randall, D. A.: Changes in External Forcings Drive Divergent AMOC
- Responses Across CESM Generations, Geophys. Res. Lett., 51, https://doi.org/10.1029/2023GL106410, 2024.
- Oh, J. H., An, S. Il, Shin, J., and Kug, J. S.: Centennial Memory of the Arctic Ocean for Future Arctic Climate
- Recovery in Response to a Carbon Dioxide Removal, Earth's Futur., 10, https://doi.org/10.1029/2022EF002804,
- 496 2022.
- 497 Oh, J. H., Kug, J. S., An, S. Il, Jin, F. F., McPhaden, M. J., and Shin, J.: Emergent climate change patterns
- 498 originating from deep ocean warming in climate mitigation scenarios, Nat. Clim. Chang., 14, 260-266,
- 499 https://doi.org/10.1038/s41558-024-01928-0, 2024.
- Park, S. W. and Kug, J. S.: A decline in atmospheric CO2 levels under negative emissions may enhance carbon
- retention in the terrestrial biosphere, Commun. Earth Environ., 3, 2–9, https://doi.org/10.1038/s43247-022-00621-
- 502 4, 2022.
- Park, S. W., Mun, J. H., Lee, H., Steinert, N. J., An, S. Il, Shin, J., and Kug, J. S.: Continued permafrost ecosystem
- carbon loss under net-zero and negative emissions, Sci. Adv., 11, 1–10, https://doi.org/10.1126/sciadv.adn8819,
- 505 2025.
- Passow, U. and Carlson, C. A.: The biological pump in a high CO2 world, Mar. Ecol. Prog. Ser., 470, 249–271,
- 507 https://doi.org/10.3354/meps09985, 2012.
- Pathirana, G., Oh, J. H., Cai, W., An, S. Il, Min, S. K., Jo, S. Y., Shin, J., and Kug, J. S.: Increase in convective
- extreme El Niño events in a CO2 removal scenario, Sci. Adv., 9, 1–10, https://doi.org/10.1126/sciadv.adh2412,
- 510 2023.
- Platt, T., Fuentes-Yaco, C., and Frank, K. T.: Spring algal bloom and larval fish survival off Nova Scotia, Nature,

- 512 423, 398–399, 2003.
- 513 Reid, P. C., Battle, E. J. V., Batten, S. D., and Brander, K. M.: Impacts of fisheries on plankton community
- 514 structure, ICES J. Mar. Sci., 57, 495–502, https://doi.org/10.1006/jmsc.2000.0740, 2000.
- Renssen, H., Goosse, H., and Fichefet, T.: Contrasting trends in North Atlantic deep-water formation in the
- 516 Labrador Sea and Nordic Seas during the Holocene, Geophys. Res. Lett., 32, 1-4
- 517 https://doi.org/10.1029/2005GL022462, 2005.
- 518 Richardson, A. J. and Schoeman, D. S.: Climate impact on plankton ecosystems in the Northeast Atlantic, Science
- 519 (80-.)., 305, 1609–1612, https://doi.org/10.1126/science.1100958, 2004.
- 520 Rogelj, J., Den Elzen, M., Höhne, N., Fransen, T., Fekete, H., Winkler, H., Schaeffer, R., Sha, F., Riahi, K., and
- 521 Meinshausen, M.: Paris Agreement climate proposals need a boost to keep warming well below 2 °c, Nature, 534,
- 522 631–639, https://doi.org/10.1038/nature18307, 2016.
- 523 Sabine, C. L., Feely, R. A., Gruber, N., Key, R. M., Lee, K., Bullister, J. L., Wanninkhof, R., Wong, C. S., R
- Wallace, D. W., Tilbrook, B., Millero, F. J., Peng, T.-H., Kozyr, A., and Ono, T.: The Oceanic Sink for
- Anthropogenic CO 2 Author(s), Rios Source Sci. New Ser., 305, 367–371, 2004.
- 526 Schmittner, A.: Decline of the marine ecosystem caused by a reduction in the Atlantic overturning circulation,
- 527 Nature, 434, 628–633, https://doi.org/10.1038/nature03476, 2005.
- 528 Schwinger, J. and Tjiputra, J.: Ocean Carbon Cycle Feedbacks Under Negative Emissions, Geophys. Res. Lett.,
- 529 45, 5062–5070, https://doi.org/10.1029/2018GL077790, 2018.
- 530 Schwinger, J., Asaadi, A., Goris, N., and Lee, H.: Possibility for strong northern hemisphere high-latitude cooling
- 531 under negative emissions, Nat. Commun., 13, https://doi.org/10.1038/s41467-022-28573-5, 2022.
- 532 Song, S. Y., Yeh, S. W., An, S. Il, Kug, J. S., Min, S. K., Son, S. W., and Shin, J.: Asymmetrical response of
- 533 summer rainfall in East Asia to CO2 forcing, Sci. Bull., 67, 213–222, https://doi.org/10.1016/j.scib.2021.08.013,
- 534 2022.
- 535 Steinacher, M., Joos, F., Frölicher, T. L., Bopp, L., Cadule, P., Cocco, V., Doney, S. C., Gehlen, M., Lindsay, K.,
- Moore, J. K., Schneider, B., and Segschneider, J.: Projected 21st century decrease in marine productivity: A multi-

- 537 model analysis, Biogeosciences, 7, 979–1005, https://doi.org/10.5194/bg-7-979-2010, 2010.
- Tong, D., Zhang, Q., Zheng, Y., Caldeira, K., Shearer, C., Hong, C., Qin, Y., and Davis, S. J.: Committed
- emissions from existing energy infrastructure jeopardize 1.5 °C climate target, Nature, 572, 373-377,
- 540 https://doi.org/10.1038/s41586-019-1364-3, 2019.
- 541 Tréguer, P., Bowler, C., Moriceau, B., Dutkiewicz, S., Gehlen, M., Aumont, O., Bittner, L., Dugdale, R., Finkel,
- 542 Z., Iudicone, D., Jahn, O., Guidi, L., Lasbleiz, M., Leblanc, K., Levy, M., and Pondaven, P.: Influence of diatom
- diversity on the ocean biological carbon pump, Nat. Geosci., 11, 27-37, https://doi.org/10.1038/s41561-017-
- 544 0028-x, 2018.
- Van Vuuren, D. P., Stehfest, E., Gernaat, D. E. H. J., Van Den Berg, M., Bijl, D. L., De Boer, H. S., Daioglou,
- V., Doelman, J. C., Edelenbosch, O. Y., Harmsen, M., Hof, A. F., and Van Sluisveld, M. A. E.: Alternative
- pathways to the 1.5 °c target reduce the need for negative emission technologies, Nat. Clim. Chang., 8, 391–397,
- 548 https://doi.org/10.1038/s41558-018-0119-8, 2018.
- Winder, M. and Sommer, U.: Phytoplankton response to a changing climate, https://doi.org/10.1007/s10750-012-
- 550 1149-2, 1 November 2012.

- Wu, P., Jackson, L., Pardaens, A., and Schaller, N.: Extended warming of the northern high latitudes due to an
- overshoot of the Atlantic meridional overturning circulation, Geophys. Res. Lett., 38, 1-5,
- 553 https://doi.org/10.1029/2011GL049998, 2011.
- Yi, X., Fu, F. X., Hutchins, D. A., and Gao, K.: Light availability modulates the effects of warming in a marine
- 555 N2 fixer, Biogeosciences, 17, 1169–1180, https://doi.org/10.5194/bg-17-1169-2020, 2020.

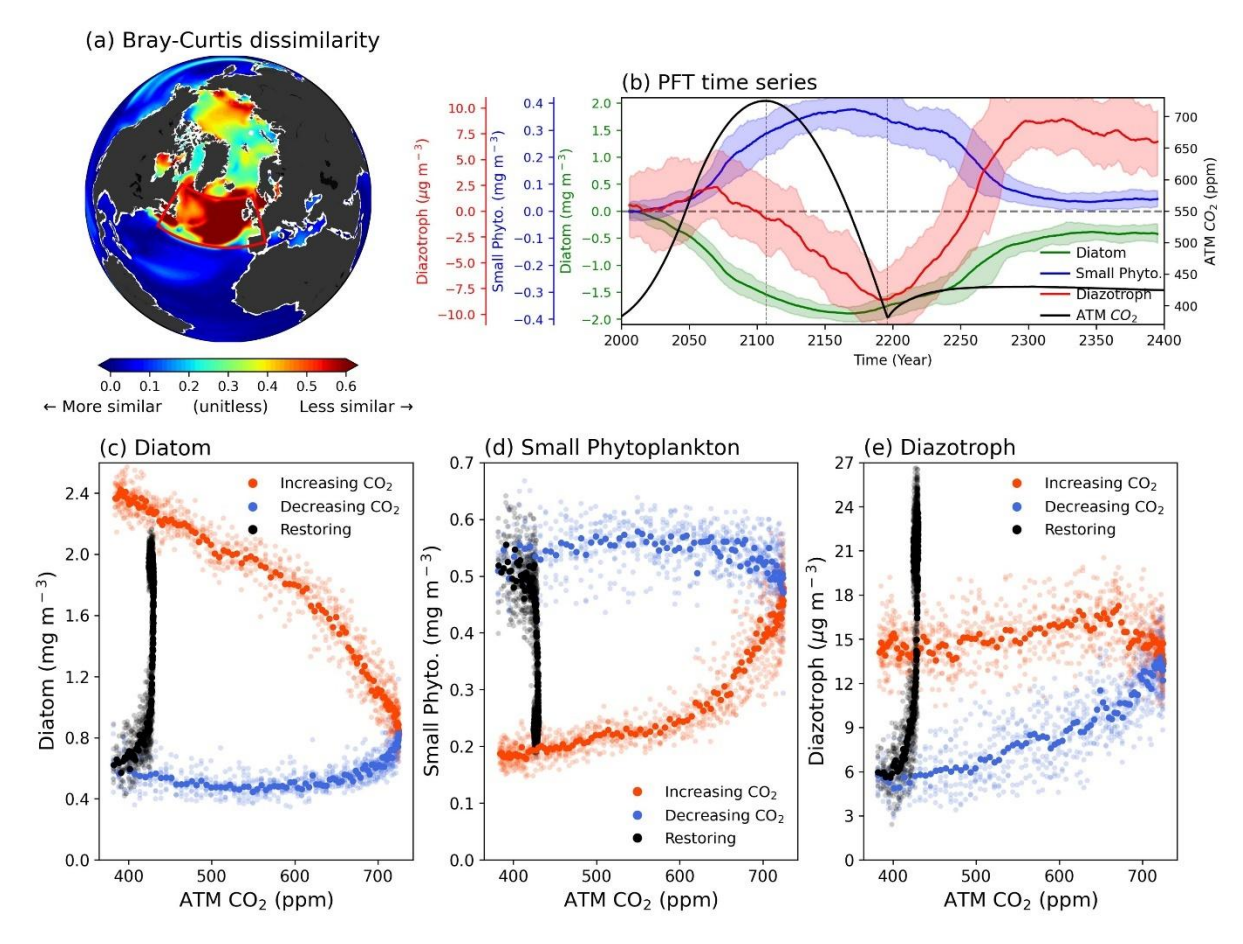


Figure 1. a, Bray-Curtis dissimilarity of phytoplankton community between climatology period and CO₂ down period. Larger values indicate a significant change in phytoplankton composition between the two periods. **b,** Time series of three phytoplankton functional types (PFTs). The colors in each plot represent atmospheric CO₂ concentration (black), diatom (green), small phytoplankton (blue), and diazotroph (red), respectively. All plots are drawn in 11-year moving averages. Shading indicates the range of minimum-maximum values between total ensembles. Changes in SPNA area-averaged biomass (y-axis) by PFTs corresponding to global mean atmospheric CO₂ concentration (x-axis) for **c,** diatoms **d,** small phytoplankton and **e,** diazotrophs. The colors in scatters indicate the 3 periods (CO₂ increasing period; orange, CO₂ decreasing period; blue, Restoring; black).

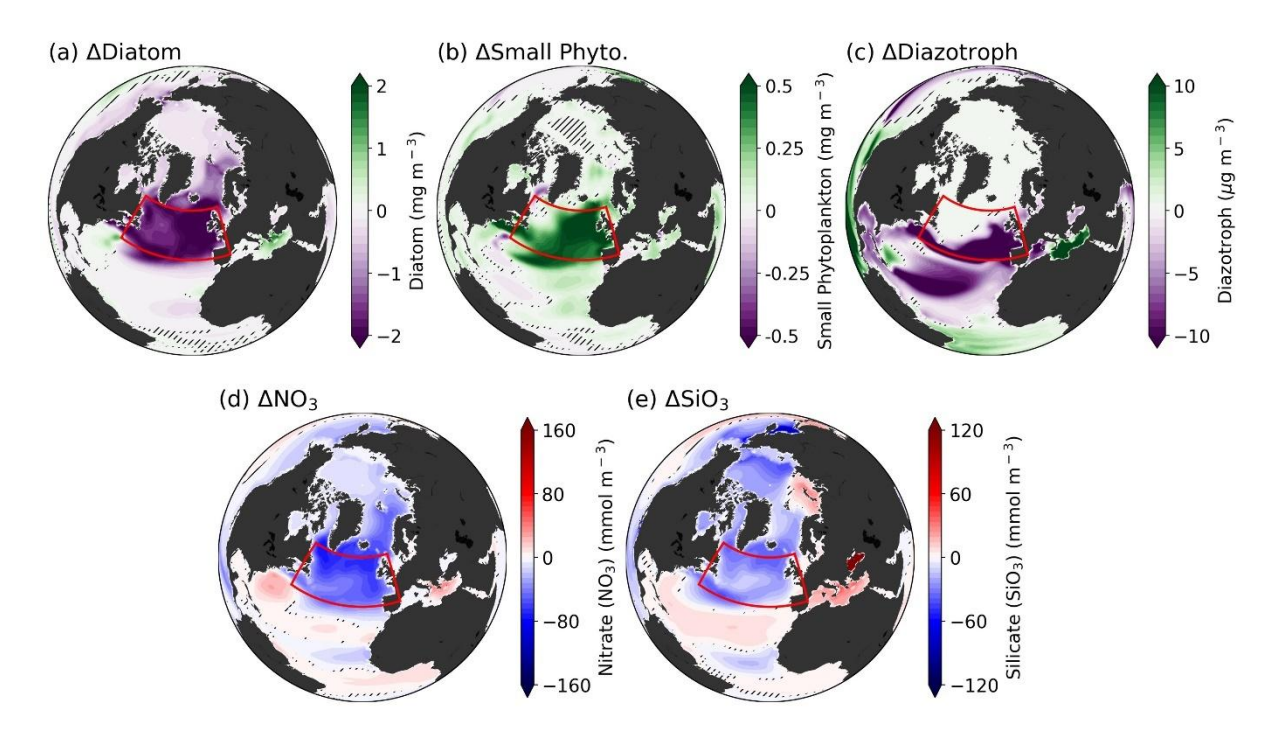


Figure 2. a-c, Differences in each PFT between CO₂ down and climatology periods **d-e,** Differences in macronutrients (NO₃, PO₄) between CO₂ down and climatology periods. Hatches indicate the non-significant region between total ensembles based on the bootstrap method.

568

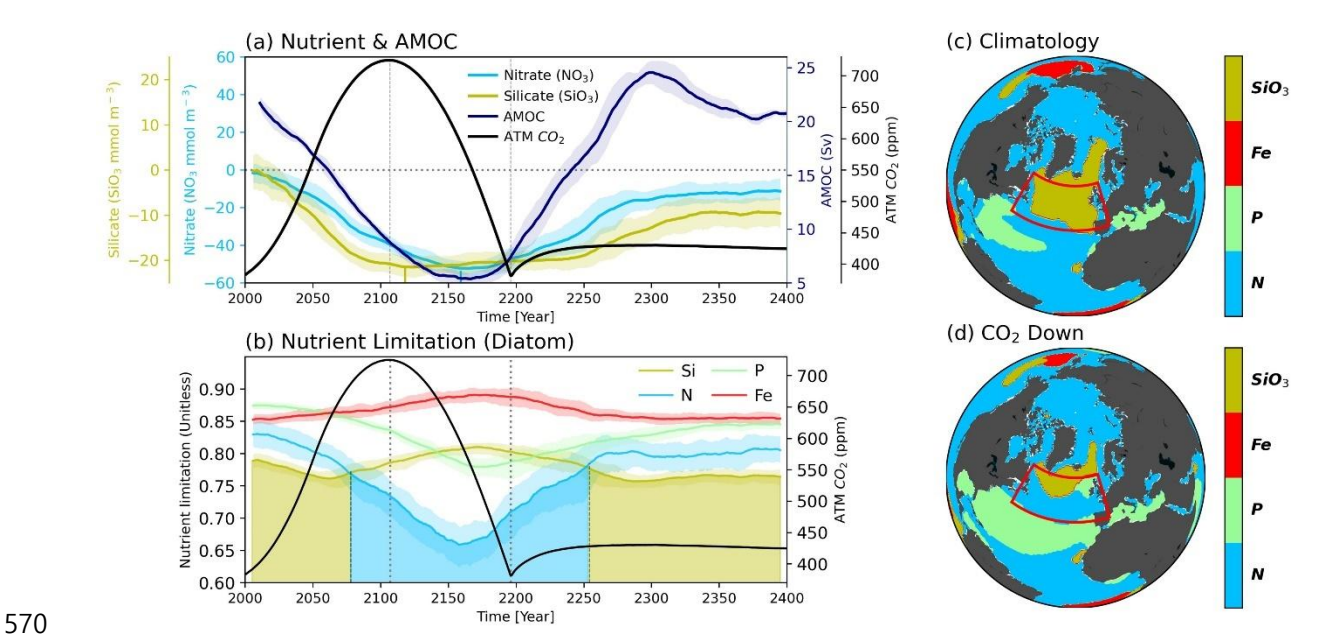


Figure 3. a, Time series of strength of Atlantic Meridional Overturning Circulation (AMOC; navy), Nitrate (NO₃; sky-blue), Silicate (SiO₃; dark-khaki) and atmospheric CO₂ concentration (black) **b,** Nutrient limitation of diatom for four nutrients (SiO₃; dark-khaki, Nitrogen (N); sky-blue, Phosphorus (P); light-green, Iron (Fe); red). All plots are drawn in 11-year moving averages and the shading indicates the range of minimum-maximum values between total ensembles. In addition, the shaded areas under the plots indicate the primary limiting nutrients for diatom growth. Nutrient limitation distribution of diatom during both **c,** Climatology and **d,** CO₂ down period.

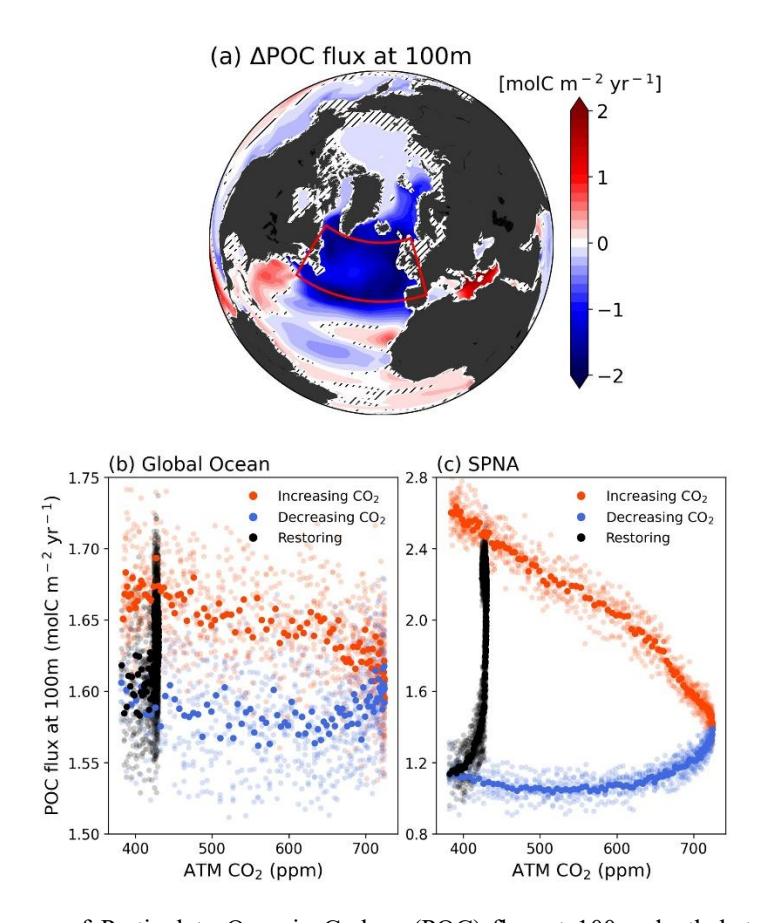


Figure 4. a, Differences of Particulate Organic Carbon (POC)-flux at 100m depth between CO₂ down and climatology periods. Changes in POC-flux at 100m depth of **b,** global ocean and **c,** SPNA region in response to CO₂ forcing. Orange color scatters indicate the CO₂ increasing period, blue scatters indicate the CO₂ decreasing period and black scatters indicate the Restoring period.